Int. J. Nanosci. Nanotechnol., Vol. 11, No. 3, Sept. 2015, pp.139-146

Study of Mesoporous Silica Nanoparticles as Nanocarriers for Sustained Release of Curcumin

A. Bolouki[1], L. Rashidi[2], E. Vasheghani-Farahani[3*] and Z. Piravi-Vanak[2]

1. Chemical Engineering Department, Islamic Azad University Shahrood Branch, Shahrood, I. R. Iran.
2. Food and Agriculture Department, Standard Research Institute, Iranian National Standards Organization, I. R. Iran.
3. Biotechnology Division, Chemical Engineering Department, Tarbiat Modares University, Tehran, I. R. Iran.

(*) Corresponding author: evf@modares.ac.ir
(Received: 20 Feb 2015 and Accepted: 10 Sep. 2015)

Abstract
Curcumin (CUR) is a hydrophobic molecule and beneficial antioxidant with known anticancer property. The bioavailability of curcumin is low because of its hydrophobic structure. Mesoporous silica nanoparticles (MSN) loaded by CUR were used as nanocarriers for sustained release of CUR in four different media such as simulated gastric, intestinal, colon and body fluids (SGF, SIF, SCF, and SBF, respectively). In this study MSN and its amine-functionalized (AP-MSN) were synthesized, loaded by CUR and then characterized by transmission electron microscopy (TEM), scanning electron microscopy (SEM), Fourier transform infrared spectroscopy (FT-IR), N_2 adsorption isotherms, X-ray diffraction (XRD) and thermal gravimetric analysis (TGA). TGA showed that the amount of CUR loaded into MSN and AP-MSN (named MSN-CUR, AP-MSN-CUR, respectively) was 1.44 and 9.5%, respectively. Entrapment efficiency of CUR in MSN and AP-MSN was found to be 3.6 and 23.75%, respectively. Release rate of CUR from AP-MSN-CUR was slower than that from MSN-CUR at different pHs of media. In addition, the release rate of CUR from AP-MSN-CUR in acidic buffer solution was slower than that in alkaline media.
Keywords*: Antioxidant, Curcumin, Mesoporous silica nanoparticles, Release.*

1. INRODUCTION

The chemical formula of Curcumin (CUR) is diferuloyl methane; 1, 7-Bis-(4-hydroxy-3-methoxyphenyl)-hepta-1, 6-diene-3, 5–dione and it is the yellow pigment in the Asian spice turmeric [1]. CUR is a hydrophobic polyphenol derived from the rhizome (turmeric) of the herb *Curcuma longa* which is used as a spice, food additives, and herbal medicine in some of the countries of Asia. CUR chemical structure is shown in Figure. 1. The *in vivo* and *in vitro* studies of CUR have shown the properties including anticancer [2], antiviral [3], anti-arthritic [1], anti-amyloid [1], antioxidant [4], anti-inflammatory [5], anti-intestinal worms [6], and anti-aging properties [1].

In addition, there are several studies on the release of CUR from different carriers. Hydrogel nanoparticles loaded by CUR were investigated as a hydrophilic carrier for delivery of CUR [2].Oral delivery of CUR by chitosan nanoparticles was studied improved the bioavailability and

chemical stability of CUR [7]. Mesoporous –type spherical hollow silica nanoparticles were used for selective immobilization of CUR onto the internal surface by covalent bonding [8].

Cationic nanoparticles of chitosan/poly (ε-caprolactone) nanoparticles loaded by CUR were prepared and enhanced the cellular uptake of CUR [9]. Single-walled carbon nanotubes (SWCNTs) loaded by CUR were prepared and then used as a novel carrier [10]. Mesoporous silica nanoparticles (MSN) could improve the bioavailability of drugs and its unique properties such as high surface area, facile modification of surface area, stability, and nontoxic structure make it a suitable carrier system [11]. MSN were also studied as a suitable carrier system for delivery of drugs [11, 12], proteins [13], vitamins [14], and antioxidants [15]. MSN surface could be modified with suitable functional groups to enhance the loading of hydrophobic or hydrophilic drugs or facilitated delivery in the body [16]. MSN were studied as suitable nanocarriers for delivery of gallic acid (GA) [17] and vitamin C [14] and low cytotoxicity of MSN was investigated on *Adipose mesenchymal* stem cells [15]. In this study, MSN were synthesized and then functionalized by 3-aminopropyltriethoxyorthosilane (APTES) (AP-MSN) for increasing of CUR loading into nanoparticles. Then, MSN and AP-MSN were loaded by CUR and named MSN-CUR and AP-MSN-CUR, respectively. The release of CUR from MSN-CUR and AP-MSN-CUR into the simulated gastric, intestinal, colon, and body fluids (SGF, SIF, SCF, and SBF, respectively) was investigated.

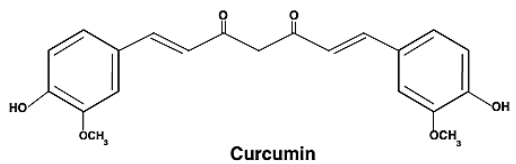

Figure1. *Chemical structure of curcumin*

2. MATERIAL AND METHODS

2.1 Materials

N-cetyltrimethylammonium bromide (CTAB), tetraethyl orthosilicate (TEOS), sodium hydroxide, 1, 3, 5-trimethylbenzene (TMB), and hydrochloric acid (HCl, 37%) and Sodium hydroxide (NaOH) were obtained from the Merck Company (Germany). Curcumin was purchased from Sigma-Aldrich Company. Simulated intestinal and colon fluids (SIF and SCF) were prepared by Imidazole buffer at pHs 7.4 and 6.8 as mentioned in our previous work [14, 15]. In addition, simulated gastric fluid (SGF) and simulated body fluid (SBF) were prepared using the method described by Rashidi *et al.* [14, 15].

2.2. Preparation of samples

2.2.1. Synthesis of large pore size mesoporous silica nanoparticles (MSN)

MSN with large pore size were prepared according to our previous work [17]. Briefly, 1 g of CTAB was dissolved in 480 ml of nano pure water and 7 ml of mesitylene (as a swelling agent) was added to the CTAB solution and the mixture was stirred for 5 h. Then 3.5 ml of 2.0 M NaOH (aq) was introduced to the CTAB solution at 80 ºC. At this temperature, TEOS (5 ml, 21.9 mmol) was added drop wise (at a rate of 1 ml/min) into the CTAB solution. The reaction mixture was stirred for 2 hours at 80 ºC. The precipitate was isolated by filtration (polypropylene filter of 0.45 µm), then washed with abundant water and ethanol. Nanoparticles were dried under vacuum at 60 ºC for 24 h. The surfactant was removed via calcination method.

2.2.2. Synthesis of amine-functionalized mesoporous silica nanoparticles

To synthesize of AP-MSN, 1 g of the large pore size of MSN dispersed in 100 ml of toluene at 50°C. Then, 1 ml of APTES was added to the reaction mixture and heated to reflux temperature followed by stirring

under nitrogen for 20 h. Nanoparticles were recovered by filtration (through a 0.45 µm polypropylene filter) and then washed with ethanol several times. The solid products were dried at 100°C for 12 h.

To measure the amount of amine groups and loading percent of CUR, thermo-gravimetric analysis (TGA) (SDT Q 600 model) was done on the functionalized nanoparticles [18].

2.2.3. Curcumin (CUR) loading

CUR loading was performed as described in previous studies [14, 15, and 17]. Briefly, 500 mg of MSN or AP-MSN was added in 10 ml of ethanol: acetone (70:30 (v/v)) solution containing 20 mg/ml CUR and then it kept in darkness while stirring at 150 rpm for 24 h. Then, CUR-loaded-nanoparticles were filtrated and washed with acetone and deionized water three times and dried under vacuum at room temperature. To measure the amount of CUR loaded into nanoparticles, 1 µl of filtrate was diluted to 10 ml by addition of ethanol: acetone (70:30 (v/v)) solvent and then analyzed using UV/Vis spectroscopy at 260 nm. CUR loading percent and entrapment efficiency were calculated by using Eqs. 1 and 2:

$$\text{CUR Loading [\%]} = 100 \times \left(\frac{W_{CUR\ loaded\ into\ AP-MSN\ or\ MSN}}{W_{CUR\ @\ AP-MSN\ or\ MSN}}\right) \quad (1)$$

$$\text{Entrapment Efficiency [\%]} = 100 \times \left(\frac{W_{CUR\ Loaded\ into\ AP-MSN or\ MSN}}{W_{Initial\ weight\ of\ CUR}}\right) \quad (2)$$

In addition, the quantity of CUR loaded into the nanoparticles was determined by TGA.

2.2.4. Mesoporous silica nanoparticles characterization

Fourier transform infrared spectroscopy (FT-IR) was performed on a Perkin Elmer spectrometer using the Kerr pellet method. Philips X'Pert multipurpose diffractometer with a thin film attachment was applied for low angle glazing incidence measurements. For this purpose, a parallel plate collimator was attached in the diffracted beam. The diffractograms were recorded over the range 1–10.0° (2θ) with a step size of 0.02° and an accumulation time of 5 s. Surface area and porosity were determined from nitrogen adsorption–desorption isotherms obtained at −196 °C (on a Micromeritics ASAP2010 analyzer). Pore size distributions were calculated from the desorption branch using the Barrett-Joyner-Halenda (BJH) method and pore volumes measured at P/P0 = 0.2-0.4. In all cases, the material was degassed at 120°C for 6 h before nitrogen adsorption. Particle morphology was analyzed by scanning electron microscopy (SEM, Philips XL-30). The structural properties and morphology of nanoparticles were studied by transmission electron microscopy (TEM, Philips CM120). Zeta potential measurement and size distribution were carried out by electrophoretic mobility using a Zetasizer 3000 (Malvern Instruments, Orsay, France) at 25 °C in buffer solutions. After counting about 150 particles, the mean size and size distribution of MSN or AP-MSN were obtained.

2.2.5 Release studies in simulated fluids

To study CUR release from MSN-CUR or AP-MSN-CUR, four different media, including SGF (HCl aqueous solution, pH 1.2), SIF (pH 6.8), SCF (pH 7.4) and SBF (pH 7.4) were prepared. 0.5 ml of acetone was mixed with 1.5 ml of each media to dissolve released curcumin. The release of CUR was determined by soaking 10 mg of MSN-CUR or AP-MSN-CUR into a vial containing 2 ml of one of the media including acetone. For each of the media, a blank was prepared and then vials were put on the shaking water bath at 37 °C and 80 rpm. The dissolution medium was sampled at a predetermined time interval, and replaced by fresh medium immediately. The supernatant was analyzed to determine the released CUR by PerkinElmer UV-Vis spectrometer at 260 nm for SGF and 265

nm for SIF and SBF. Measurements were carried out in triplicate with a standard deviation of less than 5%.

3. RESULTS

3.1. Nanoparticles characterizations

XRD patterns of MSN, MSN-CUR, AP-MSN and AP-MSN-CUR are shown in Figure. 2. It is observed that the ordered mesoporous structure of MCM-41 type MSN in the XRD patterns with four peaks (d-spacing), at (100), (110), (200) and (210) diffraction planes of synthesized nanoparticles loaded with CUR were weaker than those of unloaded nanoparticles [19].

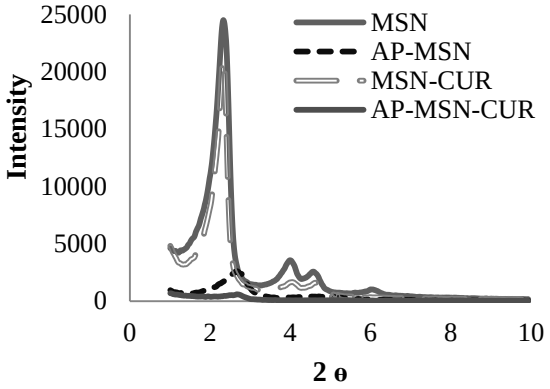

Figure2. *XRD patterns of MSN, MSN-CUR, AP-MSN, and AP-MSN-CUR*

The post grafting modification of MSN surface and curcumin loading may reduce or disappear peaks in (200) and (210) reflections because of filling the pores of nanoparticles with the functional groups or loaded curcumin. After the as-synthesized samples have been loaded with CUR, one diffraction peak was still present and the intensity of it strongly reduced. In addition, the other three diffraction peaks disappeared due to the lattice shrinkage and a loss of pore ordering in the structure of loaded MSN. TEM images of MSN and AP-MSN are shown in Figure. 3**.** The average size of MSN and AP-MSN was 110±13 nm and 135±10 nm, respectively. In addition, the histogram of MSN and AP-MSN size distribution is shown in Figure. 3. For determination of the mean size of MSN and AP-MSN, 150 particles were counted.

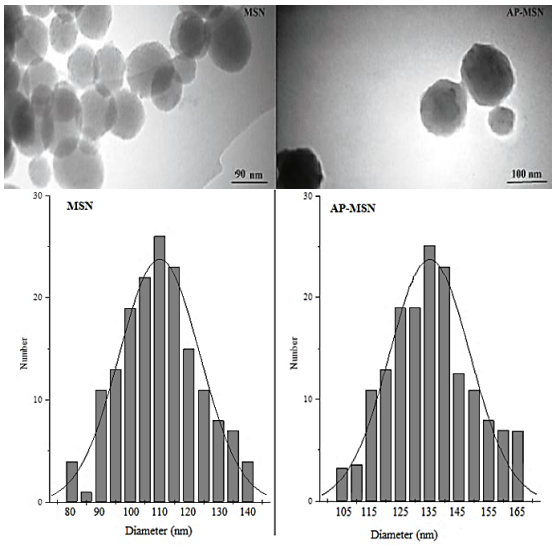

Figure3. *TEM images of MSN and AP-MSN and the histogram of MSN and AP-MSN size distribution.*

Figure 4 shows FTIR spectra of MSN, MSN-CUR, AP-MSN, and AP-MSN-CUR with characteristic vibration bands in 1620, 802, 955 and 447 cm^{-1} which correspond to Si-OH bending, Si-OH bending, Si-OH symmetrical stretching and Si-OH bending vibrations, respectively [19].

The magnitudes of these bands decreased in AP-MSN and AP-MSN-CUR because of anchoring APTES groups to the MSN surface or CUR loading. The absorption peak in the spectral range of 2950-2970 cm^{-1} can be attributed to C-H asymmetric and symmetric stretching vibrations caused by introducing methyl groups during the functionalization by APTES and this peak increased further when CUR was loaded into AP-MSN. AP-MSN showed strong bands around 1590 and 1678 cm^{-1} due to the presence of N-H and C=O bonds of APTES.

In addition, a very broad absorption band centered at 3450 cm^{-1} corresponds to Si-OH and NH_2 which increased after functionalization by APTES and clearly decreased after loading of CUR, but this peak increased in MSN-CUR due to O-H groups of CUR [20, 21]. In addition, decrease of strong 1080 cm^{-1} band was a

result of Si-O-Si stretching vibrations caused by CUR loading into the AP-MSN.

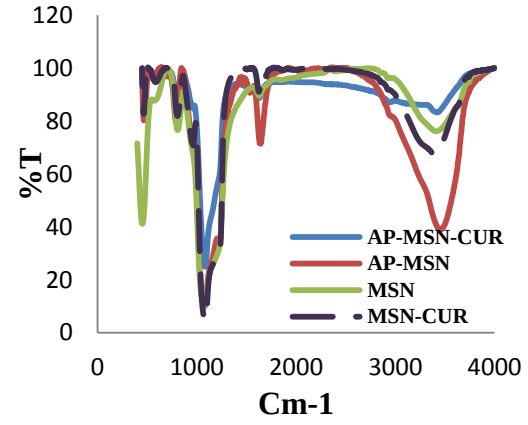

Figure4. *FTIR spectra of MSN, MSN-CUR, AP-MSN and AP-MSN-CUR.*

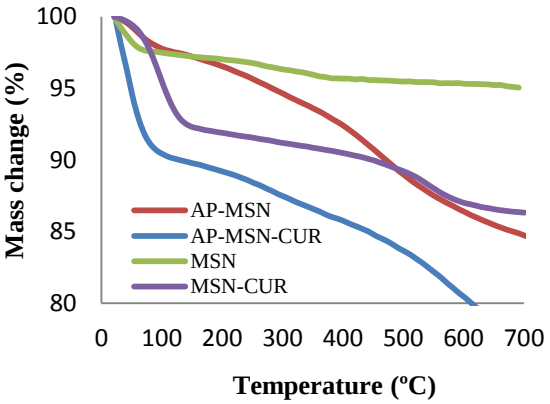

Figure5. *TGA thermograms of AP-MSN, AP-MSN-CUR, MSN and MSN-CUR*

In addition, loading capacity and entrapment efficiency of CUR into MSN and AP-MSN were determined by UV-Vis and calculated by Eq. (1-2). CUR loading capacity and entrapment efficiency were obtained 1.82 and 4.55% for MSN-CUR and, 9.75 and 24.4% for AP-MSN-CUR, respectively. In addition, TGA was performed for determination of CUR loaded into nanoparticles. TGA thermograms showed that the weight loss for AP-MSN was 12.21% because of amine group decomposition behavior (Figure. 5). The weight loss of MSN-CUR and AP-MSN-CUR as a result of CUR decomposition was 1.44 and 9.5%, respectively. It was found that CUR loading increased into AP-MSN because of the positive charge of AP-MSN surface. Mesitylene was used for increasing of pore size of nanoparticles. It was reported that the mixing time mesitylene added to the reaction mixture could play an important role in the increase of MSN pore size [17]. The pore size for two kinds of MSN, obtained by mixing of mesitylene with CTAB solution for 2 and 5 h, were 2.44 and 3.44 nm, respectively. Therefore, mesitylene was added to the reaction mixture for 5 h and then nanoparticles were characterized by N_2 adsorption isotherms. The N_2 adsorption-desorption isotherms curves of MSN, AP-MSN, MSN-CUR, and AP-MSN-CUR samples are shown in Figure. 6. As shown in this Figure, the intensity of nitrogen adsorption-desorption decreased by amine-functionalization and CUR loading into nanoparticles.

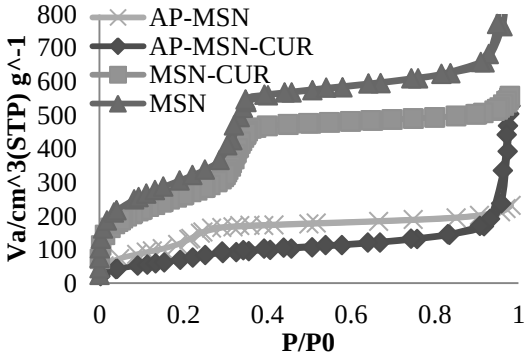

Figure6. *N_2 adsorption–desorption isotherms AP-MSN, AP-MSN-CUR, MSN and MSN-CUR*

Reduction of pore size and pore volume by functionalization of MSN, as shown in Table 1**,** are attributed to the filling of functionalized MSN pores by amine groups. In addition, the BET surface area, total pore volume, BJH adsorption volume of pores, and pore diameter in AP-MSN-CUR were lower than those in unloaded ones.

The zeta potential of AP- MSN in buffer solutions at pH 7.4, 6.8 and 1.2 was found to be -18.3, -13.2 and +50.79, respectively. In addition, the surface charge of MSN was -10.1, -14.09, and +2.64 in buffer solutions at pH 7.4, 6.8 and 1.2, respectively. Therefore, higher loading of

CUR into AP-MSN pores is related to the strong electrostatic attraction between the negative charge of CUR and the positive charge of AP-MSN surface.

Table1. *BET and BJH parameters of MSN, MSN-CUR, AP-MSN and AP-MSN-CUR*

Sample	S_{BET} (m^2/g)	Total pore volume (cm^3/g)	BJH pore diameter W_{BJH} (nm)	BJH pore volume (cm^3/g)
MSN	992.4	0.965	3.40	1.037
AP-MSN	439.5	0.357	3.28	0.313
MSN-CUR	0.944	0.899	3.31	0.998
AP-MSN-CUR	382.8	0.215	3.04	0.248

3.2. CUR release into selected media

It was reported that amine groups of AP-MSN can be protonated depending on the pH of the aqueous solution. The profile of CUR release from MSN-CUR and AP-MSN-CUR in three different pHs of media is shown in Figure 7(a)**.** These results showed that the burst release of CUR from MSN-CUR in SGF at pH 1.2 was lower than that in SIF at pH 6.8 and SCF at pH 7.4. In SGF, the burst release of CUR from AP-MSN-CUR was significantly lower than that from MSN-CUR as shown in Figures 7(a) and 7(b). MSN-CUR exhibited higher initial burst release (22.5%) within the first 0.5 h, followed by the reduced release rate during the next 23.5 h (46.3% of the loaded CUR was released) at pH 1.2 but AP-MSN-CUR exhibited lower initial burst release (14.5%) within the first 0.5 h, followed by lower release rate during the next 23.5 h (22.75% of loaded CUR was released) at pH 1.2. The release profiles at pH 6.8 show that 25.25 and 16.77% of loaded CUR released from MSN-CUR and AP-MSN-CUR within the first 0.5 h, respectively. The amount of CUR released from MSN and AP-MSN-CUR within 0.5 h was 28.25, and 17.12%, at pH 7.4, respectively.

During the next 23.5 h, the CUR released from MSN-CUR and AP-MSN-CUR was 47.17, and 38.75%, at pH 6.8 and 58.3, and 43.5% at pH 7.4, respectively. The release profile of CUR from MSN-CUR and AP-MSN-CUR in SBF is shown in Figure 7(b).

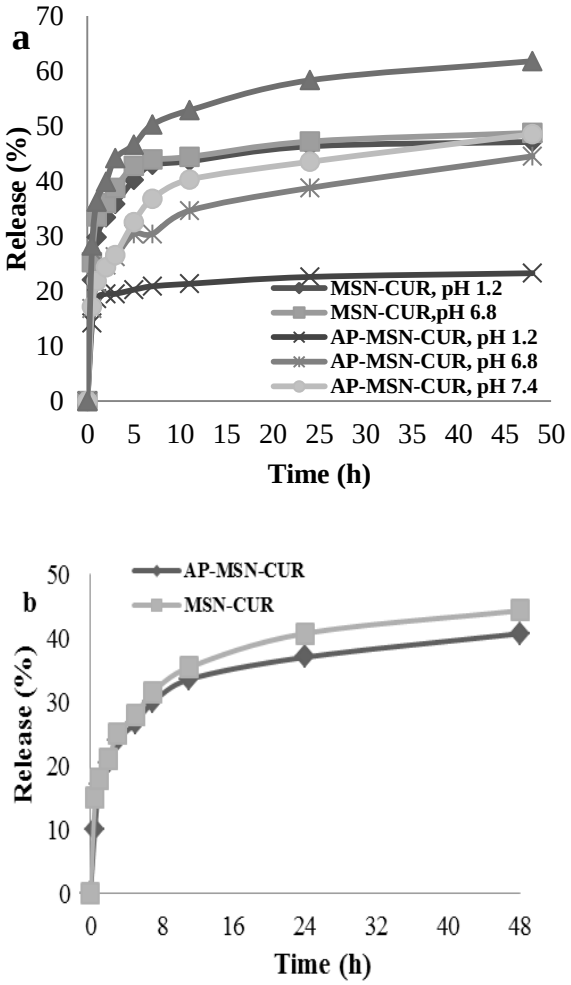

Figure7. *The release profile of CUR from MSN-CUR and AP-MSN-CUR in (a) SGF, SIF and SCF, (b) in SBF*

These results indicate that 15 and 10.1% of CUR released from MSN-CUR and AP-MSN-CUR within the first 0.5 h followed by 40.76, and 37.04% release within the next 23.5 h, respectively. The CUR release from MSN-CUR and AP-MSN-CUR was 85.72 and 50% within 240 h. These results also showed that CUR released from AP-MSN-CUR into SGF, SIF, SCF and SBF was slower than that of MSN-CUR. The release rate of CUR from AP-MSN-CUR in an acidic solution was slower than that in an alkaline solution because of the negative charge of CUR and higher positive charge of AP-MSN in acidic solution that leads to slower release of CUR.

4. DISCUSSIONS

Curcumin is a low molecular weight polyphenol that has been found as an interesting molecule due to its suitable potential for inhibition of chemically induced carcinogenesis in the skin, fore stomach, colon, esophageal, ovarian, bone, pulmonary, brain, cervical, prostate, kidney, hepatic, pancreatic, bladder and colorectal cancer [1]. In the recent years many carriers have been identified for safe delivery of CUR in the body. For example, curcumin-loaded soybean phospholipids liposomes nanoparticles were used as a promising transdermal carrier for curcumin in cancer treatment [20]. The CUR loading capacity was 82.33% and release of CUR was obtained 67.38% in PBS (at pH 6.5) after 24 h. Bombyx mori silk (BMS) nanofibers loaded by CUR were produced by electrospinning. The release rate of CUR from CUR loaded- silk nanofibers (CSNFs) was fast and about 90% of CUR released during 24 h in the alkaline pH [21]. CUR loaded-carboxymethyl chitosan (O-CMC) reported as a suitable carrier for CUR in the body. Entrapment efficiency and loading capacity of CUR in O-CMC nanoparticles were found to be 87% and 48%, respectively. The release rate of CUR at pH 4.5 and 7.4 reached about 52 and 58% after 120 h, respectively [22]. Encapsulating efficiency of CUR by chitosan- tripolyphosphate (TPP) nanoparticles was 75 ± 2%. 52.41 and 98.91% of physically loaded CUR from CUR loaded- chitosan- TPP nanoparticles released at pH 7.4 and 5.4, respectively, after 96 h [23]. In this work, MSN and AP-MSN counterparts were used as carriers for delivery of CUR. We provided the evidence that CUR could be loaded into MSN and AP-MSN pores. Loading of CUR increased as a result of functionalization of MSN surface by APTES. The spherical shape and surface characteristics of the synthesized MSN and AP-MSN, as shown in Figure 3, indicated that the particle size of synthesized MSN and AP-MSN was suitable for intracellular uptake. It was found that the burst release and the release rate of CUR into SGF reduced by functionalization of MSN. In addition, the interaction of the hydrogen bonds between the CUR molecules and the release medium was relatively weaker in SGF than SIF or SCF. By decreasing pH to 1.2, a strong electrostatic interaction was generated between modified silanol groups on the surface of AP-MSN and CUR molecules which resulted in the reduction of CUR release into SGF.

5. CONCLUSION

It was noticed that many parameters such as steric effects, space of the adsorption sites of CUR and its hydrophobicity might affect loading of CUR into MSN-CUR or AP-MSN-CUR.

The sustained release of CUR molecules from AP-MSN-CUR in an acidic buffer solution was obtained. Results showed that encapsulation of CUR into AP-MSN protect CUR in the acidic pH. It was found that mesoporous silica nanoparticles could be suitable carriers for CUR. The surface of these nanoparticles could be modified with the suitable functional groups and used for delivery of CUR in the body.

REFERENCES

1. A. R. Mullaicharam, A. Maheswaran, Int. J. Nutr. Pharm. Neuro. Dis, Vol. 2, (2012), pp. 92-99.
2. Teong B., Lin C-Y., Chang S-J., Niu G. C-C., Yao C-H., Chen J-F., Kuo S-M., J. Mater. Sci. Mater. Med, Vol. 26, (2015), 49.
3. A. Mazumber, K. Raghavan, J. Weinstein, K.W. Kohn, Y. Pommer. Biochem Pharmacol., Vol. 49, (1995), pp. 1165–1170.
4. A. Barzegar, A. A. Moosavi-Movahedi, Plos One., Vol. 6, (2011), pp. 26012.
5. M. Venkata, R. Sripathy, D. Anjana, N. Somashekara, Am. J. Infect. Disease, Vol. 8, (2012), pp. 26-33.
6. G.C. Jagetia, B.B. Aggarwal. J. Clin. Immunol., Vol. 27, (2007) 20–35.

7. F. Akhtar, M. Moshahid, A. Rizvi, S. K. Kar, Biotech. Adv., Vol. 30, (2012), pp. 310–320.
8. D. Jin, K.W. Park, J. H. Lee, K. Song, J.G. Kim, M. L. Seo, J. H. Jung, J. Mater. Chem., Vol. 21. (2011), pp. 3641-3645.
9. J. Liu, L. Xu, C. Liu, D. Zhang, S. Wang, Z. Deng, W. Lou, H. Xu, Q. Bai, J. Ma, Carbohydrate Polymer., Vol. 90. (2012), pp. 16- 22.
10. L. Haixia, N. Zhang, Y. Hao, Y. Wang, S. Jia, H. Zhang, Y. Zhang, Z. Zhang. Drug Deliv, (2013), PP. 1–9.
11. He Q, Shi J, J. Mater. Chem. Vol. 21, (2012), pp.5845–5855
12. F. Tang, L. Li, D. Chen, Adv. Matter., Vol. 24. (2012), pp. 1504-1534.
13. I.I. Slowing, J.L. Vivero- Escoto, C.W. Wu, V.S.Y. Lin, Adv. Drug Del. Rev., Vol. 60, (2008), pp. 1278–1288.
14. L. Rashidi, E. Vasheghani- Farahani, K. Rostami, F. Gangi, M. Fallahpour. Iran J. Biotech. Vol. 11, (2013), pp. 209-213.
15. L. Rashidi, E. Vasheghani-Farahani, M. Soleimani, A. Atashi K. H. Rostami, F. Ganji, M. Fallahpour, M. T. Tahouri, J. Nanopart. Res. Vol. 16, (2014), pp. 2285 -6.
16. T. Xia, M. Kovochich, C. Liong, ACS Nano., Vol. 3, (2009), pp. 3273–3286.
17. L. Rashidi, E. Vasheghani- Farahani, K. Rostami, F. Gangi, M. Fallahpour., Asia-Pacific. J Chem. Eng., *(*2014), PP. 1832.
18. Y. Zhang, Z. Zhi, T. Jiang, J. Zhang, Z. Wang, S. Wang, J. Control. Release. Vol. 145, (2010), pp. 257–263.
19. .Z. Li, K. Su, B. Cheng, Y. Deng, J. Colloid Interface Sci. Vol. 342, (2010), pp. 607–613.
20. Y. Chen, O. Wu, Z. Zhang, L. Yuan, X. Liu, L. Zhou, Molecules. Vol. 17, (2012), pp. 5972-5987.
21. T. Elakkiya, G. Malarvizhi, S. Rajiv, T. S. Natarajan, Polym, Int, Vol. 63, (2014), pp.100–105.
22. A. Anitha, S. Maya, N. Deepa, K.P. Chennazhi, S.V. Nair, H. Tamura, R. Jayakumar, Carbohydrate Polymers Vol. 83, (2011), pp. 452–461.
23. R. Mirnejad, M.A. Mofazzal Jahromi, S. Al-Musawi, M. Pirestani, M. Fasihi Ramandi, K. Ahmadi, H. Rajayi, Z. M. Hassan, M. Kamali, Iran J Biotech, Vol. 12, (2014), p. e1012.